

# FIRST EXPERIMENTAL OBSERVATIONS OF THE PLASMA-CASCADE INSTABILITY IN THE CeC PoP ACCELERATOR

I. Petrushina<sup>1</sup>, Y. Jing<sup>1</sup>, V. N. Litvinenko<sup>1</sup>, J. Ma, I. Pinayev, K. Shih<sup>1</sup>, G. Wang<sup>1</sup> Y.H. Wu<sup>1</sup>  
Brookhaven National Laboratory, Upton, NY, USA  
<sup>1</sup>also at Stony Brook University, Stony Brook, NY, USA

## Abstract

Preservation of the beam quality is important for attaining the desirable properties of the beam. Collective effects can produce an instability severely degrading beam emittance, momentum spread and creating filamentation of the beam. Microbunching instability for beams traveling along a curved trajectory, and space charge driven parametric transverse instabilities are well-known and in-depth studied. However, none of the above include a microbunching longitudinal instability driven by modulations of the transverse beam size. This phenomenon was observed for the first time during the commissioning of the Coherent electron Cooling (CeC) Proof of Principle (PoP) experiment [1, 2]. Based on the dynamics of this instability we named it a Plasma-Cascade Instability (PCI). PCI can strongly intensify longitudinal micro-bunching originating from the beam's shot noise, and even saturate it. Resulting random density and energy microstructures in the beam can become a serious problem for generating high quality electron beams. On the other hand, such instability can drive novel high-power sources of broadband radiation. In this paper we present our experimental observations of the PCI and the supporting results of the numerical simulations.

## PLASMA-CASCADE INSTABILITY

The PCI is a microwave instability occurring in beams which propagate in a straight line, and is driven by modulation of the electron beam density via transverse focusing. The resulting modulation of the frequency of the plasma oscillations can result in a strong exponentially growing longitudinal instability.

Let us consider a cold, homogeneous infinite electron beam of density  $n$ . A small perturbation of the beam density,  $\delta n \ll n$ , will cause oscillations within the beam with plasma frequency  $\omega_p = \sqrt{\frac{4\pi n e^2}{m}}$ , which can be described by the equation of plasma oscillations:

$$\frac{d^2 \tilde{n}}{dt^2} + \omega_p^2 \tilde{n} = 0, \text{ with } \tilde{n} = n + \delta n \quad (1)$$

Assume that the beam is propagating through a periodic focusing lattice consisting of 5 solenoids, or 4 focusing cells (see Fig. 1). We will denote the period of this lattice to be  $2l$ , and the solenoid strengths are defined such that it supports a periodic nature of the beam envelope  $a$ . The system of solenoids provides a periodic transverse beam size modulation, which causes a periodic modulation of the beam density. This density modulation will be inversely

proportional to the square of the beam radius  $a$ , which would lead to a corresponding modulation of the plasma frequency. Modulation of the plasma frequency is shown in green, and its maxima fall onto the minima (waist) of the transverse beam envelope. These plasma oscillations will lead to the subsequent modulation of the longitudinal density of the beam.

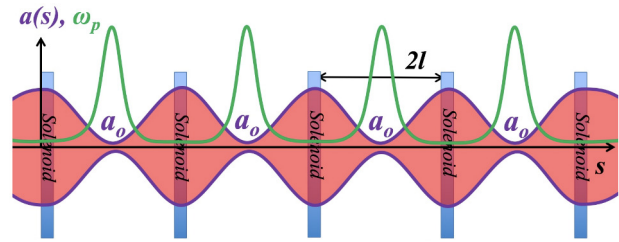


Figure 1: A sketch of four focusing cells with periodic modulations of beam envelope,  $a(s)$  (purple with red shading), and the plasma frequency,  $\omega_p$  (green). Beam envelope has waists,  $a_0$ , in the middle of each cell where plasma frequency peaks. Scales are adjusted for illustration purpose.

When the oscillator frequency is modulated with a period close to a half of oscillation period, it results in an exponential growth of oscillation amplitude: the phenomenon known as parametric resonance, which leads to an instability.

The set of two coupled second order differential equations (see Eq. 2) gives a complete description of the PCI: the transverse envelope equation and the equation for the longitudinal density modulation  $\tilde{q}_k$ .

$$\begin{cases} \frac{d^2 \hat{a}}{d\hat{s}^2} - \frac{k_{sc}^2}{\hat{a}} - \frac{k_{\beta}^2}{\hat{a}^3} = 0, \\ \frac{d^2 \tilde{q}_k}{d\hat{s}^2} + \frac{2k_{sc}^2}{\hat{a}^2} \tilde{q}_k = 0 \end{cases} \quad (2)$$

Here we utilize a set of dimensionless parameters inherited from [3], with normalized beam envelope  $\hat{a} = \frac{a}{a_0}$ , where  $a_0$  is the beam waist;  $\hat{s} = \frac{s}{l}$  is the longitudinal distance  $s$  normalized to the half of the lattice period. The beam envelope inside the cell is fully determined by the two dimensionless parameters: the space charge,  $k_{sc} = \sqrt{\frac{2}{\beta^3 \gamma^3} \frac{I_0 l^2}{I_a a_0^2}}$ , and the geometric (or emittance),  $k_{\beta} = \frac{\epsilon l}{a_0^2}$ . Here we denote the beam current as  $I_0$ , and  $I = \frac{mc^3}{e}$  is the Alfvén current.

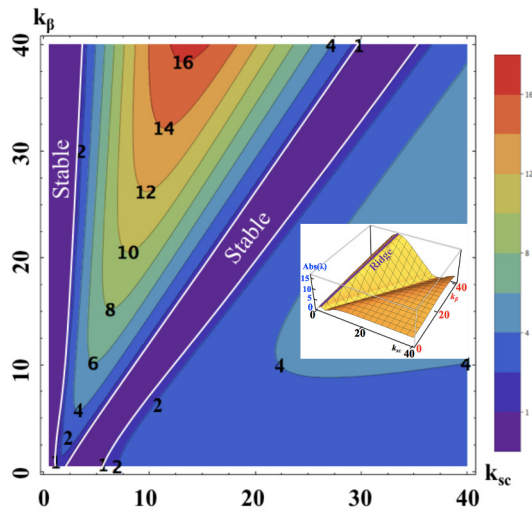


Figure 2: Contour plots of the absolute value of the growth rate per cell. Purple area highlighted by white lines indicates the areas of the stable oscillations. Density modulation grows exponentially outside these areas. The 3D form of this graph in the inset shows clearly identifiable ridge along the  $k_\beta = 3(k_{sc} - 1.2)$  line, where the growth rates peak.

Figure 2 demonstrates the growth rate in one cell of the system which depends on the above mentioned parameters. The plot defines the stable and unstable regions of the solution, indicating that the growth rate peaks along the  $k_\beta = 3(k_{sc} - 1.2)$ . A complete description of the PCI theory can be found in [3,4].

## EXPERIMENTAL OBSERVATIONS

In order to study the PCI experimentally we utilized the existing accelerator used to deliver electron beams for the CeC PoP experiment. The layout of the accelerator is shown in Fig. 4. The electron bunches with duration of 400 ps are generated in the 1.25 MV 113 MHz SRF photoinjector [5]. The RF curvature from the photogun is then compensated by the use of two normal conducting RF cavities, which allow us to reduce the energy spread within the beam to a 0.01% level. The six solenoids in the Low Energy Beam Transport (LEBT) section provide the desired strong-focusing aperiodic lattice for the PCI demonstration. To detect the presence of a density modulation within the beam, we attempted to study the longitudinal beam profile by utilizing the combination of the 45° dipole and the off-crest operation of the 5-cell 704 MHz SRF cavity. Due to the lack of a dedicated beamline for diagnostics, we established operation of the 5-cell cavity at zero crossing with low accelerating voltage of  $V \sim 100\text{-}200$  kV, which allowed us to correlate particle's energy with the arrival time. The dipole and the profile monitor located in the dogleg served as the energy spectrometer.

Figure 3 demonstrates a clear dependence of the PCI on the beam charge: the structures vanish below 100 pC, and enhance with increased charge.

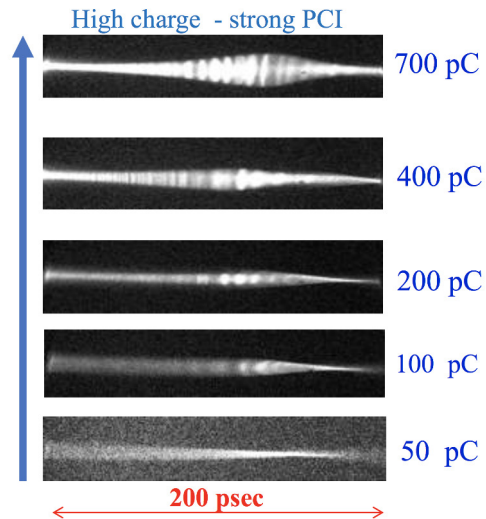


Figure 3: A set of randomly selected structures measured for uncompressed electron bunches with charge ranging from 50 pC to 700 pC per bunch.

The post-processing of several randomly selected time profiles measured for various beam charges from 0.45 to 0.7 nC clearly indicated a strong density modulation along the beam. The fast Fourier transformation (FFT) of the time profiles showed a good agreement with the result of simulations performed with the code SPACE [6, 7], and demonstrated a prominent peak at 0.4 THz. The fact that the noise profiles are not repeatable confirms that the modulation must originate from the electron beam itself, rather than from the laser structures or the induced wake fields. The calculated correlation function of the AC part of the density modulation clearly indicated that the modulation is caused by a broad-band micro-bunching instability.

For the CeC operation we were compressing 400 psec electron bunches with a charge of 0.7-1.4 nC to a peak current of 50-100 A. This required  $\sim 20$ -fold compression of the electron beam, which proportionally shifted the frequency of the density modulation to around 10 THz.

## SUPPRESSION OF THE PCI

The PCI, due to its nature, exhibits a strong dependence on the transverse focusing in the LEBT section and, therefore, can be eliminated by adjusting the lattice accordingly.

Figure 5 shows the comparison between the radiation power spectra obtained for the lattice used during the CeC PoP demonstration experiment and a so-called relaxed lattice specifically designed for noise suppression. These results were obtained using IMPACT-T [8], the simulation was carried out for the complete CeC beamline including the effects of the wake fields. The narrow  $\delta$ -like spikes at frequencies of 15 and 20 THz in the spectra of the relaxed setting (red) correspond to a computational artifact related to the choice of the mesh and time step. The result clearly demonstrates that the PCI can be suppressed at the frequencies around

Content from this work may be used under the terms of the CC BY 3.0 licence (© 2019). Any distribution of this work must maintain attribution to the author(s), title of the work, publisher, and DOI

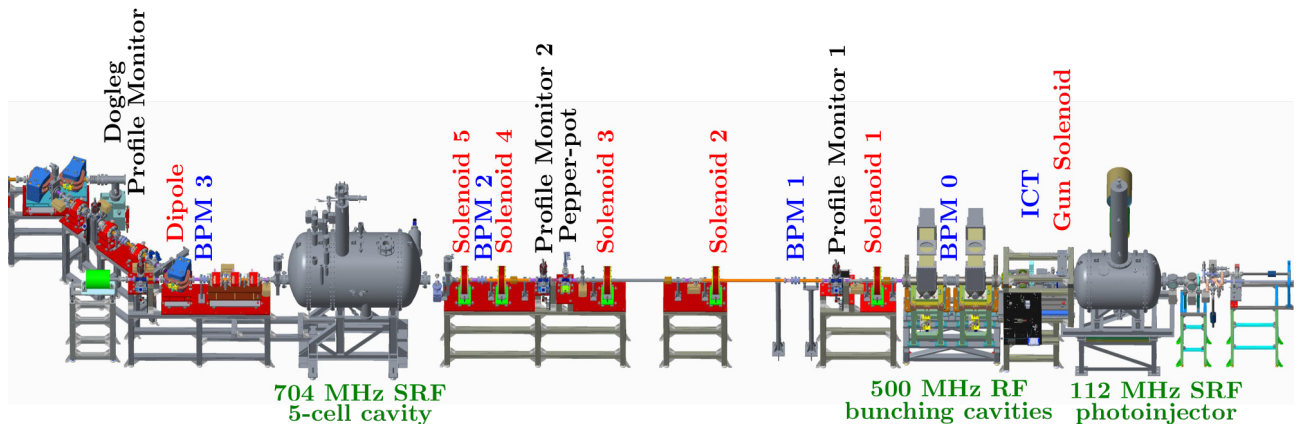


Figure 4: CeC PoP electron accelerator used for the PCI study.

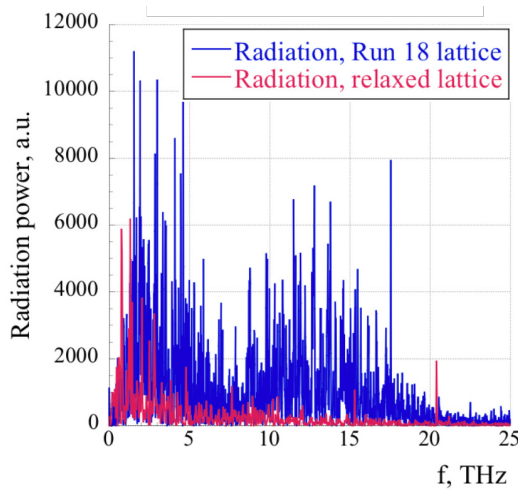


Figure 5: Radiation spectrum of the compressed 0.7 nC electron bunch at the exit of the SRF linac simulated by IMPACT-T for standard CeC lattice (blue) and relaxed lattice (red).

10 THz, when compared to the radiation power spectra for the regular lattice.

We dedicated our experiment in 2019 to the extensive study of the PCI suppression with the goal to demonstrate the ability to deliver a quiet beam with the noise level applicable for the future cooling experiments. The IR detector was installed at the end of the beamline for the characterization of the synchrotron radiation in the THz range from the bending magnet due to the longitudinal density modulation in the beam.

The baseline of the radiation was established for a slightly (4-fold) compressed beam in a relaxed LEBT lattice. Averaged over 4 long scans, the lock-in amplifier signal for the baseline was found to be about 145 V/C. After the noise level was determined, several optimization studies were performed where we observed the effects of the LEBT solenoid settings and buncher voltage on the dipole radiation. We explored numerous combinations of parameters to achieve the lowest possible signal.

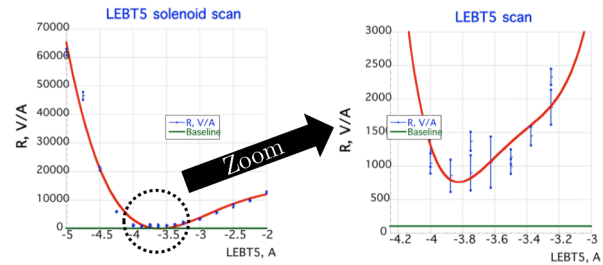


Figure 6: IR signal as a function of current in LEBT 5 solenoid.

The minimal goal for the experiment was to demonstrate that the ratio of the noise from the PCI to the shot noise in the electron beam can be reduced to 100 and below. As a result of the lattice optimization we were able to achieve a noise level exceeding the shot noise by only a factor of 4 to 10 for a large range of the lattices. The optimized set-up has a flat response of the noise on the variation of the solenoid current leaving sufficient headroom for optimization of other beam parameters. An example of a solenoid scan is shown in Fig. 6.

## CONCLUSION

A complete theoretical description of the PCI was developed and supported through simulations. The suppression of the PCI in the LEBT section of the CeC accelerator was demonstrated experimentally and confirmed by simulations. The required noise level necessary for the future CeC demonstration experiment was achieved. Moreover, the PCI was utilized as a base of the future Plasma-Cascade Amplifier for the upcoming CeC PoP experiment in 2020 [3].

## ACKNOWLEDGMENTS

This work is supported by Brookhaven Science Associates, LLC under Contract No. DEAC0298CH10886 with the U.S. Department of Energy, DOE NP office grant DE-FOA-0000632, and NSF grant PHY-1415252.

## REFERENCES

- [1] V.N. Litvinenko and Ya.S. Derbenev, “Coherent electron cooling”, *Phys. Rev. Accel. Beams*, vol. 102, p. 114801, 2009.
- [2] I. Pinayev *et al.*, “Performance of CeC PoP Accelerator”, in *Proc. 10th Int. Particle Accelerator Conf. (IPAC'19)*, Melbourne, Australia, May 2019, pp. 559–561. doi:10.18429/JACoW-IPAC2019-MOPMP050
- [3] V.N. Litvinenko *et al.*, “Plasma-Cascade micro-bunching Amplifier and Coherent electron Cooling of a Hadron Beams”, *arXiv preprint arXiv:1802.08677*, 2018.
- [4] V.N. Litvinenko *et al.*, “Plasma-Cascade Instability— theory, simulations and experiment”, *arXiv preprint arXiv:1902.10846*, 2019.
- [5] I. Petrushina *et al.*, “High Brightness CW Electron Beams From Superconducting RF Photoinjector”, presented at the North American Particle Accelerator Conference (NAPAC'19), Lansing, Michigan, September 2019, MOZBB4, this conference.
- [6] X. Wang *et al.*, “AP-Cloud: Adaptive Particle-in-Cloud method for optimal solutions to Vlasov–Poisson equation”, *Journal of Computational Physics*, vol. 316, pp. 682–699, 2019.
- [7] K. Yu and V. Samulyak, “SPACE Code for Beam-Plasma Interaction”, in *Proc. 6th Int. Particle Accelerator Conf. (IPAC'15)*, Richmond, VA, USA, May 2015, pp. 728–730. doi:10.18429/JACoW-IPAC2015-MOPMN012
- [8] “IMPACT-T: A 3D Parallel Particle Tracking Code in Time Domain”, <https://amac.lbl.gov/~jiquiang/IMPACT-T/index.html>.